Point spread functions of photons in time-resolved transillumination experiments using simple scaling arguments

Victor Chernomordik, Ralph Nossal, and Amir H. Gandjbakhche
Division of Computer Research and Technology, Physical Sciences Laboratory, National Institutes of Health, Bethesda, Maryland 20892

(Received 28 May 1996; accepted for publication 30 July 1996)

Simple scaling arguments are used to determine spatial resolution achievable in time-resolved transillumination experiments involving highly diffuse media. These arguments allow us to obtain relationships linking target resolution at different planes inside an optically turbid slab to the gating times of the imaging system. We show that this approach yields the same results as those obtained previously from an approximate and rather complicated analytical derivation. In addition, we are now able to assess the effects of scattering anisotropy on spatial resolution attainable when gating times are so short that a constant scaling of photon transport scattering length is not appropriate. These results should enable one to devise more accurate and simpler image reconstruction algorithms.

I. INTRODUCTION

Spectral imaging of deep tissue structure, using nonionizing visible and near-infrared radiation, has attracted widespread interest as a potential method for noninvasive detection of tumors.[1–3] Because light incident on most biological tissues is multiply scattered within a distance of 1 mm and thus rapidly becomes diffuse, conventional transillumination techniques lead to very poor resolution of deeply lying abnormalities.[4] Time-gated transillumination, by selecting only short-path photons which have small deviation from the optical axis, can improve the spatial resolution.

However, the improved resolution occurs at the cost of lower detected intensity,[5–7] so clinically useful imaging requires a balance between the intensity of the detected light and the spatial resolution. For this reason it is important to understand how the resolution depends on optical parameters, gating time, tissue thickness, and the depth at which an object lies below the tissue surface. Moreover, it is now clear that imaging of an optically abnormal embedded target in otherwise normal tissue requires complex image reconstruction algorithms utilizing descriptions of the spatial spread of photon trajectories within the tissue.[8,9] Because the resolution is defined in terms of the spatial spread, the following work, on obtaining simple and accurate analytical relations relating the resolution to the gating time of a transillumination imaging system, also is important to the broader question of devising inverse imaging algorithms.

In this paper we present a new derivation that is much simpler than methods previously used to study questions of resolution.[10,11] In addition to yielding results for interior targets which are in agreement with previous expressions, it also provides an expression that accurately represents the resolution for targets located near the periphery of a slab. Furthermore, we obtain an expression that is valid at short times, which should be applicable to the analysis of transport through slabs whose thickness is but a few times the inverse of the transport-corrected mean-free path. By assuming that photon diffusion inside the tissue sample is isotropic, we first derive simple expressions that adequately represent transillumination time-resolved imaging resolution (with coaxial source and detector) over the whole range of depths. We then present an analysis of spatial resolution for the more general case of anisotropic random walks, valid for short times where constant scaled cross sections generally cannot be used.

II. ANALYSIS FOR AN ISOTROPIC SCATTERING MODEL

As in our previous work,[10] we formulate the problem in terms of a photon random walk on a discrete rectangular lattice having isotropic transition probabilities, and later convert to real experimental parameters. Time and position are given, respectively, in terms of the number of steps n and the dimensionless indices $\{x,y,z\}$. Here we consider that the source and detector are pointlike, which means that the finite size of the source and detector are not taken into account; effects of the size of the detector are analyzed elsewhere (see, e.g., Ref. 12).

The principal quantity for determining both the resolution and intensity of time-resolved imaging is the probability $\Gamma(\rho,\Delta n|z)$ that a photon emerging on the opposite side of the slab of thickness L after a total of $L+\Delta n$ steps (Δn is the "excess number of steps") will, as it crosses the plane at depth z below the sample surface, be at a radial distance ρ from the $\{x,y\}$ axis passing through the source (i.e., the point of photon insertion). We neglect the possible refractive index mismatch between the tissue and its surrounding media, so the interfaces of the slab are taken to be nonreflecting. To a first approximation this is a valid assumption because our main goal is to describe the resolution associated with relatively short photon paths; reflected photons, if important, contribute only to intensities associated with photons which

move for longer times within the tissue. The expression for $\Gamma(\rho,\Delta n|z)$ represents the point spread function (PSF) of the corresponding time-gated image of objects at depth z.

An analytical expression, based on random walk theory,[13,14] previously was derived for this characteristic at the midplane.[10] Derived for the case of an equivalent isotropic scattering medium, it has the following rather complicated form:

$$\Gamma\left(\rho,\Delta n|z=\frac{1}{2}\right)=\frac{9}{16\pi^{5/2}(\Delta n)^{3/2}}\sum_{k=-\infty}^{\infty}\sum_{m=-\infty}^{\infty}\left[\frac{\alpha_1(k)^{1/2}+\alpha_1(m)^{1/2}}{\alpha_1(k)^{1/2}\alpha_1(m)^{1/2}}\,e^{-[\alpha_1(k)^{1/2}+\alpha_1(m)^{1/2}]^2/\Delta n}\right.$$
$$\left.-2\frac{\alpha_1(k)^{1/2}+\alpha_2(m)^{1/2}}{\alpha_1(k)^{1/2}\alpha_2(m)^{1/2}}\,e^{-[\alpha_1(k)^{1/2}+\alpha_2(m)^{1/2}]^2/\Delta n}+\frac{\alpha_2(k)^{1/2}+\alpha_2(m)^{1/2}}{\alpha_2(k)^{1/2}\alpha_2(m)^{1/2}}\,e^{-[\alpha_2(k)^{1/2}+\alpha_2(m)^{1/2}]^2/\Delta n}\right], \tag{1}$$

where

$$\alpha_1(k)=\frac{3}{2}\left[\rho^2+\left[\frac{L}{2}-1+2kL\right]^2\right],$$
$$\alpha_2(k)=\frac{3}{2}\left[\rho^2+\left[\frac{L}{2}+1+2kL\right]^2\right]. \tag{2}$$

However, it was shown by computer curve fitting that these PSFs are well represented by Gaussian distributions, whose standard deviations, $\{\sigma\}$, can be taken as measures of spatial resolution. These Gaussian fits lead to a simple empirical formula for σ

$$\sigma=0.406(\Delta n)^{1/2}, \tag{3}$$

when σ is expressed[10] in units of mean effective scattering length (i.e., μ_s^{-1}). Because the dimensionless random walk parameters Δn, ρ, L, and σ can be related to actual time and space variables r and t through the scattering coefficient μ_s as

$$\Delta n=\mu_s c\Delta t,\quad \rho=\frac{\mu_s r}{\sqrt{2}},\quad L=\frac{\mu_s d}{\sqrt{2}}+1 \tag{4}$$

(where d is the actual thickness, c is the speed of light, and the quantity Δt is the excess time by which a photon is delayed in reaching the detector when compared with the direct time of flight through the slab), the standard deviation may be written in terms of experimentally accessible parameters as[10]

$$\Delta x_\sigma=0.406\left(\frac{c\Delta t}{\mu_s}\right)^{1/2}. \tag{5}$$

In a related study,[11] an empirical formula relating resolution as a function of depth to the resolution at the half-plane [see Eq. (3)] also was found, viz.,

$$\sigma(z)=\sigma(L/2)\cdot f_0(z), \tag{6}$$

where $f_0(z)=1-2.35(Z^*-0.5)^2$, and Z^* is the fractional depth defined as $Z^*=(z-1)/(N-1)$. This formula agrees well with results of numerical calculations for a broad range of depths. However, discrepancies between Eq. (6) and the $\{\sigma\}$ obtained by fitting the generated expressions by Gaussians are significant near the input and output surfaces. We now show that the empirical functional form given by Eq. (6) indeed is correct. Moreover, we derive an improved, analytic expression for $f_0(z)$ that is valid even near the boundaries of the slab.

We first note that the mean-square distance $\langle\Delta r^2\rangle$ traveled in an n-step isotropic random walk is $\langle\Delta r^2\rangle=n$, where $\langle\Delta r^2\rangle$ is expressed in units of root-mean-square of the run length distribution.[15] In the case of an isotropic three-dimensional medium, the mean-square distances projected onto the x,y,z axes evidently are equal to $\langle\Delta x^2\rangle=\langle\Delta y^2\rangle=\langle\Delta z^2\rangle=n/3$. It follows that, for photons that emerge from the output slab surface at $z=L$ after Δn extra steps, the mean-square displacement in a direction parallel to slab surface when at the depth z is

$$\langle\Delta x^2\rangle|_z=\tfrac{1}{3}(\Delta n)(z/L),\quad \text{for } z\leq L/2. \tag{7}$$

In particular, we have for the midplane ($z=L/2$),

$$\langle\Delta x^2\rangle|_{L/2}=\tfrac{1}{6}(\Delta n). \tag{8}$$

If the number of random steps is large, then, according to the central-limit theorem, the distribution of photon displacements in any direction parallel to the slab surface is close to Gaussian

$$\phi(\Delta x)\sim\exp\left[-\frac{(\Delta x)^2}{\langle\Delta x^2\rangle}\right]. \tag{9}$$

We observe that $\phi(\Delta x)$ can be considered as the transmission directivity pattern $\phi_b(\Delta x)$ of the photon source.[16] The PSF of any imaging process can be represented as a product of transmission and reception directivity patterns

$$\mathrm{PSF}_x=\phi_b(\Delta x)\cdot\phi_r(\Delta x). \tag{10}$$

The function $\phi_r(\Delta x)$ is easily determined in our case, since the directivity pattern is a reciprocal process having the same form for transmission and reception. (When the input and output points are interchanged the random walk is exactly reversible.) However, the expected dispersions of both patterns prove to be the same only in the case of the slab midplane $z=L/2$. In this particular case, the resulting standard deviation of the PSF in the x direction, when expressed in terms of mean run length, is equal to

$$\sigma_x|_{L/2}=(\tfrac{1}{6})^{1/2}(\Delta n)^{1/2}=0.408(\Delta n)^{1/2}. \tag{11}$$

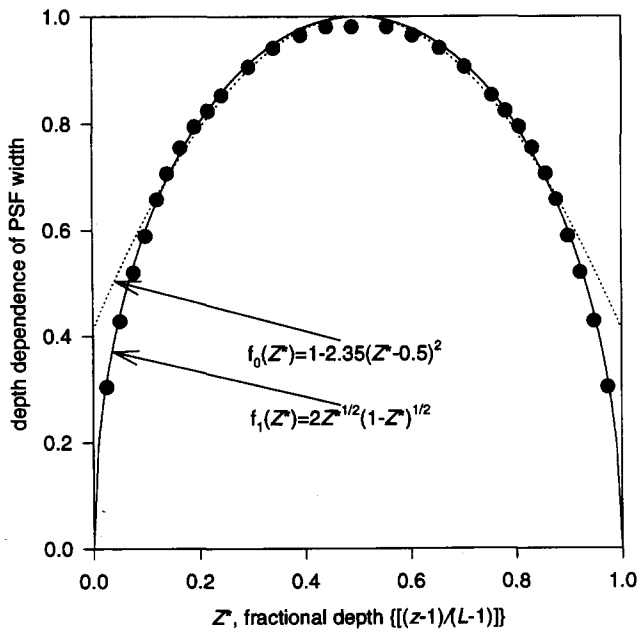

FIG. 1. Depth dependence of PSF width as a function of Z^* defined as $(z-1)/(L-1)$. Circles are the widths, σ, of Gaussian fits to the PSFs given in Ref. 11. The solid line is the functional form $f_1(Z^*)$ given in Eq. (13), and the dashed line is the empirical fit obtained in Ref. 11, $f_0(Z^*)$ [see Eq. (6)].

This formula is the same as found earlier[10] from the curve-fitting procedure, except for a negligible difference in the numerical coefficient (0.406, which was established empirically, instead of the value 0.408 obtained above from theoretical considerations).

We also can improve the empirical relation given by Eq. (6). First note that, from Eq. (7), we see that, for the reception directivity pattern, one should replace z in the formula for $\langle \Delta x^2 \rangle|_z$ by $L-z$ (the distance between the considered interior plane and the detector). Referring to Eq. (10) we then see that, for arbitrary depth z, the PSF can be expressed as

$$\mathrm{PSF}_x(z) \sim \exp[-(x^2(1/\langle \Delta x^2 \rangle|_z + 1/\langle \Delta x^2 \rangle|_{L-z}))]. \quad (12)$$

The standard deviation (which will be greatest at the midplane) is thus given at arbitrary depth as

$$\sigma(z) = \sigma(L/2) \cdot f_1(Z^*), \quad (13)$$

where, as expected, $f_1(Z^*) = 2(Z^*)^{1/2}(1-Z^*)^{1/2}$ is symmetrical relative to the midplane. The function $f_1(z/L)$ is represented in Fig. 1, where numerical data[11] are also shown for comparison. Agreement is very good (not worse than 3%) over the whole range of depths. Also shown (dotted line) is the empirical approximation given by Eq. (6).

III. EFFECT OF ANISOTROPIC SCATTERING

The anisotropy coefficient, g, in diffusionlike processes is defined as the mean cosine of the azimuthal scattering angle, θ, viz.,

$$g = \langle \cos\theta \rangle = \frac{\int_0^\pi P(\theta) \cos\theta \sin\theta \, d\theta}{\int_0^\pi P(\theta) \sin\theta \, d\theta}. \quad (14)$$

The value $g=0$ corresponds to isotropic scattering, and $g=1$ holds for complete forward scattering. Diffusionlike theories are usually derived for isotropic scattering and the effects of anisotropy are taken into account by defining a "transport-corrected scattering length" dependent on g. For example, in the diffusion approximation of photon transport theory, the transport-corrected scattering cross section is defined as $\mu_s' = \mu_s(1-g)$, regardless of scattering length distribution.

In previous work we have shown that the scaling relationships for anisotropic random walks depend on the probability distribution of the scattering lengths.[15] A general relationship between the mean square displacement and the number of steps undergone by the random walker was obtained[15] as the following function of g,

$$\langle (\Delta x)^2 \rangle = \frac{2}{3} \Delta n \left(\frac{\langle l^2 \rangle}{2} + \langle l \rangle^2 \frac{g}{1-g} \right) - \frac{2}{3} \langle l \rangle^2 \frac{g(1-g^{\Delta n})}{(1-g)^2}, \quad (15)$$

where $\langle l \rangle$ is the first moment (i.e., the mean) and $\langle l^2 \rangle$ is the mean-squared value of the run length distribution. Note that for isotropic random walks, for which $g=0$, a considerable simplification occurs [viz., $\langle (\Delta x)^2 \rangle = \Delta n \langle l^2 \rangle / 3$].

For a Poisson distribution of unit mean scattering length, which corresponds to a random distribution of scattering centers with the medium with $\langle l \rangle = 1$ and $\langle l^2 \rangle = 2$, one finds

$$\langle (\Delta x)^2 \rangle = \frac{2}{3} \Delta n \left(\frac{1}{1-g} \right) f(g, \Delta n), \quad (16)$$

where $f(g,\Delta n)$ is defined as

$$f(g,\Delta n) = \left[1 - \frac{g(1-g^{\Delta n})}{(1-g)\Delta n} \right]. \quad (17)$$

At very large Δn, where $f \to 1$, one thus obtains

$$\langle (\Delta x^2) \rangle = \frac{2}{3} \frac{\Delta n}{1-g}. \quad (18)$$

As previously mentioned [see Eqs. (2)–(5)], one needs to relate the standard deviation, σ, to a measure of resolution given in terms of experimentally accessible parameters. If we were to start with Eq. (18) we would obtain an expression identical to that given in Eq. (5), except that μ_s would be replaced by the familiar transport-corrected scattering cross section μ_s' [see discussion following Eq. (14)]. However, it is evident from Eqs. (16) and (17) that the scaling depends in a complicated way on the number of steps Δn taken by the photons. If one merely were to scale the scattering coefficient μ_s by $(1-g)$ in Eq. (4) to obtain an equivalent isotropic diffusion process, there would be an underestimation of the "transport-corrected" mean square displacement at short times. Thus one must start with the scaling of Δn obtained from Eq. (16), which is now $(1-g)/f(g,\Delta n)$ instead of $(1-g)$. However, $\langle \Delta x \rangle$ and Δn in Eq. (16) are dimensionless parameters. If one expresses the resolution in terms $\mu_s(1-g)$ (variable used in diffusionlike transport pro-

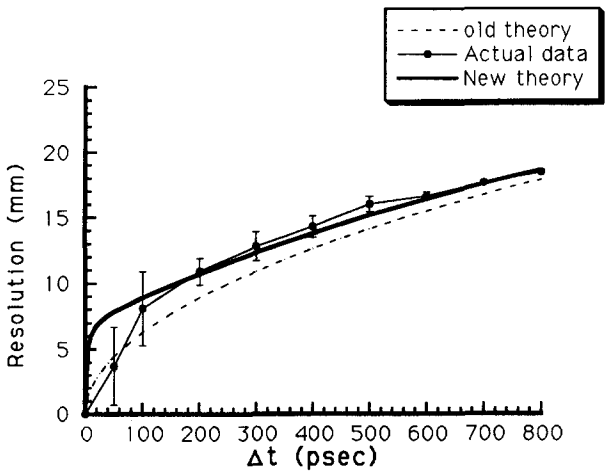

FIG. 2. Spatial resolution (filled circles with error bars), Δx_σ, as a function of excess transit time, Δt, calculated from the edge response function as reported in Ref. 17. Theoretical predictions using Eq. (19) without the correction factor (dashed line), and using the correction factor for short excess transit time (solid line) are also shown. The optical parameters of the tissue phantom are[17] $\mu_s = 10\ \text{mm}^{-1}$, $c = 0.225$ mm/ps, and $g = 0.92$.

cesses), and then uses the new scaling for Δn in real variables according to Eq. (4), one gets

$$\Delta x_\sigma = 0.408\left(c\Delta t \Big/ \mu_s(1-g) \times\left[1-\frac{g(1-g^{\mu_s(1-g)c\Delta t})}{(1-g)^2\mu_s c\Delta t}\right]\right)^{1/2}. \quad (19)$$

One can see from Eq. (19) that, for very large Δt, the scaling $\mu_s' = \mu_s(1-g)$ holds. In addition, Eq. (19) shows that, in reality, poorer resolution is obtainable at small Δt than is predicted by using the asymptotic expression for the scaling based on Eq. (18).

We have compared resolutions obtained from time-gated transillumination experiments[17] with the newly derived expression given in Eq. (19). In these experiments $\mu_s = 10\ \text{mm}^{-1}$, the refractive index of the medium is 1.33 which yields $c = 0.225$ mm/ps, and $g = 0.92$ so $\mu_s' = 0.8\ \text{mm}^{-1}$. Experimental resolutions were calculated from the edge response functions of the abrupt edge of an opaque mask embedded in the middle of the slab (51 mm thick). The resolving power of the imaging system was set to 2.91σ, which leads to a factor 1.19 (instead of 0.408) in Eq. (19). Details of the experimental setup and the procedure for calculating actual resolutions as a function of the gating times are reported elsewhere.[17] Experimental results are presented in Fig. 2 as circles with error bars. The upper curve (solid line) is calculated according to Eq. (19) with the factor 1.19, while the lower curve (dashed line) represents the same expression when the quantity is square brackets is set equal to 1, i.e., when constant scaling of the scattering coefficient is used. Clearly, a better fit of the data is obtained when the effect of anisotropy is taken into account. Although for very short gating times (less than 50 ps, corresponding to $\Delta n \approx 9$) the new approach still gives a poor description of the spatial resolution, this behavior may reflect the fact that the corresponding photons do not have enough time to follow diffusivelike paths inherent to the model used in the analysis presented above.

IV. COMMENTS

We have shown here how expressions for the resolution achievable in diffuse transillumination imaging, previously derived by semi-empirical arguments,[10] can be obtained from first principal considerations of photon random walks.[15] In addition to substantiating previous theory,[10,17] we here derived a modification that accounts for the directional persistence of a photon that arises from anisotropic scattering. The resulting expression gives yet better agreement with experimental results, for all except very short times.

We also note that the implementation of image reconstruction algorithms for embedded tissue objects requires a description of the spread of photon paths within the tissue. The perturbation in those paths caused by the presence of an abnormal target is closely related to the point spread function (PSF) of light traveling through the medium. Our simple scaling arguments enables replacement of the complicated PSF expression of Eq. (1) by its Gaussian counterpart, as given in Eq. (10). This can enormously simplify image reconstruction algorithms. Our analysis should enable one to correctly account for effects of anisotropic diffusion.

[1] B. Chance and R. Alfano, editors, *Time Resolved Spectroscopic Imaging in Tissues*, Proc. Soc. Photo-Opt. Instrum. Eng. **1431** (1991).
[2] B. Chance and R. Alfano, editors, *Photon Migration and Imaging in Random Media and Tissues*, Proc. Soc. Photo-Opt. Instrum. Eng. **1888** (1993).
[3] R. Alfano, editor, *Advances in Laser and Light Spectroscopy to Diagnose Cancer and Other Diseases*, Proc. Soc. Photo-Opt. Instrum. Eng. **2135** (1994).
[4] B. Monsees, J. M. Destouet, and D. Gersell, "Light scan evaluation of nonpalable breast lesion," Radiology **163**, 467–470 (1987).
[5] J. C. Hebden and R. A. Kruger, "Transillumination imaging performance: A time of flight imaging system," Med. Phys. **17**, 351–356 (1991).
[6] K. M. Yoo, Q. Xing, and R. R. Alfano, "Imaging objects hidden in highly scattering media using femtosecond second-harmonic generation," Opt. Lett. **16**, 1019–1021 (1991).
[7] M. D. Duncan, R. Mahon, L. L. Tankersley, and J. Reintjes, "Time-gated imaging through scattering media using stimulated Raman amplification," Opt. Lett. **16**, 1868–1870 (1991).
[8] S. R. Arridge, "Photon measurement density functions Part I," Appl. Opt. **34**, 7395–7409 (1995).
[9] D. A. Boas, M. A. O'Leary, B. Chance, and A. G. Yodh, "Scattering of diffuse photon density waves by spherical inhomogeneities within turbid media: analytical solutions and applications," Proc. Nat. Acad. Sci. (USA) **91**, 4887–4891 (1994).
[10] A. H. Gandjbakhche, R. Nossal, and R. F. Bonner, "Resolution limits for optical transillumination of abnormalities deeply embedded in tissues," Med. Phys. **21**, 185–191 (1994).
[11] A. H. Gandjbakhche, R. Nossal, and R. F. Bonner, "Theoretical studies of resolution limits of time-resolved transillumination of human breast," in *Advances in Laser and Light Spectroscopy to Diagnose Cancer and Other Diseases*, edited by R. Alfano, Proc. Soc. Photo-Opt. Instrum. Eng. **2135**, 176–185 (1994).
[12] J. A. Moon and J. Reintjes, "Image resolution of multiply scattering light," Opt. Lett. **19**, 521–523 (1994).
[13] R. F. Bonner, R. Nossal, S. Havlin, and G. H. Weiss, "Model of photon migration in turbid biological media," J. Opt. Soc. Am. A **4**, 423–432 (1987).

[14]A. H. Gandjbakhche, G. H. Weiss, R. F. Bonner, and R. Nossal, "Photon pathlength distributions for transmission through optically turbid slabs," Phys. Rev. E **48**, 810–818 (1993).

[15]A. H. Gandjbakhche, R. F. Bonner, and R. Nossal, "Scaling relationships for anisotropic random walks," J. Stat. Phys. **69**, 35–53 (1992).

[16]V. N. Adrov and V. V. Chernomordik, "Simulation of two-dimensional ultrasonic imaging of biological tissues in the presence of phase aberrations," Ultrason. Imag. **17**, 27–43 (1995).

[17]J. C. Hebden and A. H. Gandjbakhche, "Experimental validation of an elementary formula for estimating spatial resolution for optical transillumination imaging," Med. Phys. **22**, 1271–1272 (1995).